International Journal of Ecology and Environmental Sciences 48: 317-331, 2022
ISSN: 2320-5199 (Online); https://doi.org/10.55863/ijees.2022.0107

Hyperspectral Remote Sensing for Mapping Foliar Pigment Concentration in Mudumalai Tiger Reserve, India

B.S.P.C. KISHORE[1], AMIT KUMAR[1]*, PURABI SAIKIA[2] AND MOHAMMED LATIF KHAN[3]

[1]Department of Geoinformatics, Central University of Jharkhand, Ranchi-835205, India
[2]Department of Environmental Sciences, Central University of Jharkhand, Ranchi-835205, India
[3]Dr. Harisingh Gour Vishwavidyalaya (A Central University), Sagar-470003, Madhya Pradesh, India
E-mail: bspckishore@gmail.com; amit.kumar@cuj.ac.in, amit.iirs@gmail.com; purabi.saikia@cuj.ac.in; khanml61@gmail.com
ORCHID IDs: (BSPCK): 0000-0003-1835-3595; (AK): 0000-0002-4582-5677; (PS): 0000-0001-5481-282X; (MLK): 0000-0001-6849-0307

***Corresponding Author**

ABSTRACT

The present study focuses on mapping and identification of the pigment concentration and dominant invasive species in Mudumalai Tiger Reserve (MTR), Tamil Nadu, India using optical (Sentinel 2A) and hyperspectral (Hyperion) earth observation satellite images. The Hyperion satellite data-based study exhibited dominance of dense vegetation (40.64%) and moderate vegetation (27.81%), in contrast to low vegetation (15.71%) in MTR. While vegetation indices based analysis demonstrated more accurate results of forest cover through Modified Red Edge Normalised Difference Vegetation Index (MRENDVI) compared to other vegetation indices. The dominance of moderate Normalised Difference Vegetation Index (NDVI) values (0.55–0.6) were observed in MTR with moderate carotenoid concentration (<0.3) and low anthocyanin concentration (<0.2). The study highlights the prominence of *Lantana camara, Parthenium hysterophorus*, *Prosopis juliflora, and Chromolaena odorata* in the Mudumalai Tiger Reserve. The correlation of species and foliar pigment concentration provides a better understanding of the species distribution in tropical deciduous forests in southern India. The study highlights better results in Sentinel 2A images compared to Hyperion images in LULC classification due to higher spatial resolution, while Hyperion images provide more improved classification and diversity for species characterisation due to high spectral agility. The study necessitates concurrent monitoring of invasion in forest-rich regions through the adoption of potential forest conservation and management plans.

Key words: Hyperion, Sentinel 2A, Spectral Indices, Foliar Pigment.

INTRODUCTION

Tropical forests are of global importance as they are one of the most species rich terrestrial ecosystems and due to their role in biogeochemical cycles (Kothandaraman et al. 2020). Tropical forests are subject to a wide range of ecological disturbances of varied duration, intensity, and frequency (Chazdon 2003). Both natural and human-induced disturbances are quite pervasive in tropical forests (Whitmore and Burslem 1998) due to the high level of human dependence on natural forests for a range of livelihood opportunities (Kumar and Saikia 2020). Invasive species can modify natural ecosystems in terms of their structure, composition, and functioning through their extremely high propagation across the entire landscapes with or without human interventions (Asner et al. 2008). They are responsible for the unprecedented ecosystem damage and enormous economic loss (Pimentel et al. 2000). The rapid global expansion of invasive species is homogenizing the world's flora and fauna and is the second largest cause of global biodiversity loss after habitat loss and destruction (Czech and Krausman 1997, Wilcove and Chen 1998, Saikia et al. 2017).

Remote sensing plays an vital role in mapping and monitoring tropical forests over larger areas compared to the existing field-based techniques, especially with the recent launch of improved sensors, processing and modelling techniques, in combination with field data (Arockraj et al. 2015, Kishore et al. 2020). The new generation of hyperspectral, hyperspatial, and hypertemporal sensors is responsible for the rapid and innovative advancements in the perspectives of tropical forests

structure, composition, and functioning over broad spatial and temporal scales (Chambers et al. 2007). Identification of invasive weeds in a diversified landscape is very much difficult and challenging by using multispectral imagery (Dewey et al. 1991) due to their uniform spectral responses for invasives and other dominant species in the VIS and NIR wavelength regions in healthy vegetation due to comparable anatomical structure (Woolley 1971). Hyperspectral imagery is considered as one of the best alternatives to multispectral imagery (Ustin et al. 2004). With the availability of the continuous spectra inherent of species in hyperspectral imagery, it may be utilised to differentiate the species into taxonomic levels because of greater information content in terms of high spectral fidelity (Asner and Vitousek 2005). Hyperspectral observations are made up of many precisely spaced, contiguous measurements (wavebands) that provide far more information about objects than broadband multispectral observations (Kokaly et al. 2003, Lawrence et al. 2006). Hyperspectral data provide a lot of information about the biophysical and chemical characteristics of the analysed vegetation as it constitutes a source of ongoing information about spectral reflection (Trietz and Howarth 1999). Compared to multispectral remote sensing data, the classification of hyperspectral data is more complex given the wide dimension of data, the amount of training data samples, *etc*. (Chutia et al. 2020), through the uniqueness of spectral bands provide distinctive and important properties of vegetation canopy. The new machine learning algorithms including Spectral Angle Mapper (SAM) and Support Vector Machine (SVM) are popularly used for species classification of broad-leaved evergreen and coniferous tree species in western Himalayas (George et al. 2014). On the other hand, the factor-based ranking approach showed improved results (R^2 of 0.85) in discriminating mangrove species using SVM classification (Ashokkumar and Shanmugam 2014). Hyperion data was used to discriminate agricultural crops using linear discriminant analysis (LDA) and SVM in the Google Earth Engine cloud computing platform achieving overall accuracies between 75 to 95% (Aneece and Thenkabail 2018). The mapping of invasion in a heterogeneous grasslands ecosystem of Southern Ontario (Canada) using high resolution hyperspectral images (HrHSI) exhibited high separability in spectral and textural aspects between the two invading species and between invasive species and native plants, with high accuracy (~89.6%) (Dao et al. 2021).

Chlorophylls (Chl a and Chl b) are essential pigments for the conversion of solar energy to stored chemical energy and the foliar concentrations of chlorophylls often control the carbon fixed per unit radiation intercepted (Dawson et al. 2003). Chlorophylls govern the quantity of solar radiation absorbed by the leaf and influence the photosynthesis capabilities and thereby primary productivity (Filella et al. 1995). The chemical structure of the chlorophyll contains a substantial percentage of total leaf nitrogen, and numerous research has shown the exact indirect assessment of plant nutritional status in foliar chlorophyll levels (Moran et al. 2000). Carotenoids are the second major group of plant pigments, composed of carotenes and xanthophylls, which are essential structural components of the photosynthetic antenna and reaction centre complexes (Bartley and Scolnik 1995). Due to their distinctive physical and photographic characteristics, several particular and essential physiological activities have been assigned to carotenoids, including the structural role to be played in organising photosynthetic membranes, involvement in light harvesting, energy transfer, quenching and interception of deleterious free oxygen and possibly deleterious free oxygen (Edge et al. 1997). Chlorophylls and carotenoids concentration significantly increase during the growing season (Porcar-Castell et al. 2008) and it is higher for healthy and growing trees than for declining and age-old trees (Zarco-Tejada et al. 2018). In contrast, anthocyanins are frequently occurring pigments in higher plants and responsible for their red colouration and in leaves it localizes in vacuoles of epidermal cells or those just below the adaxial epidermis, but occasionally, also in the cells of the abaxial epidermis, palisade, and spongy mesophyll (Gould et al. 2008). Anthocyanins are a common component of all leaves and they can be the dominant pigment group for certain species or in particular phenological stages (Gitelson et al. 2001). Anthocyanins have the ability to regulate photosynthesis and limit photoinhibition and photobleaching through modifying the light

environment within a leaf (Barker et al. 1997), thereby having a photoprotective function (Steyn et al. 2002, Close and Beadle 2003). Considering the complexity of the forest species composition, and their relation with invasive species in the tropical deciduous forest of southern India, an attempt has been made to study the forest species identification using hyperspectral remote sensing technology and its association with invasive species in the parts of Mudumalai Tiger Reserve.

STUDY AREA

The parts of Mudumalai Tiger Reserve has been taken up as the study area (comprising 390.84 km^2), which is located between 11°18' to 11°47' N latitude and 76°25' to 76°36' E longitude having an elevation ranging from 05 to 2451m (Fig. 1). The area is connected to the Sigur Reserve Forest in the east located along the river Moyar, while the Nilgiri hills in the south. Built-up land is primarily concentrated in the northern and central parts in small fragments.

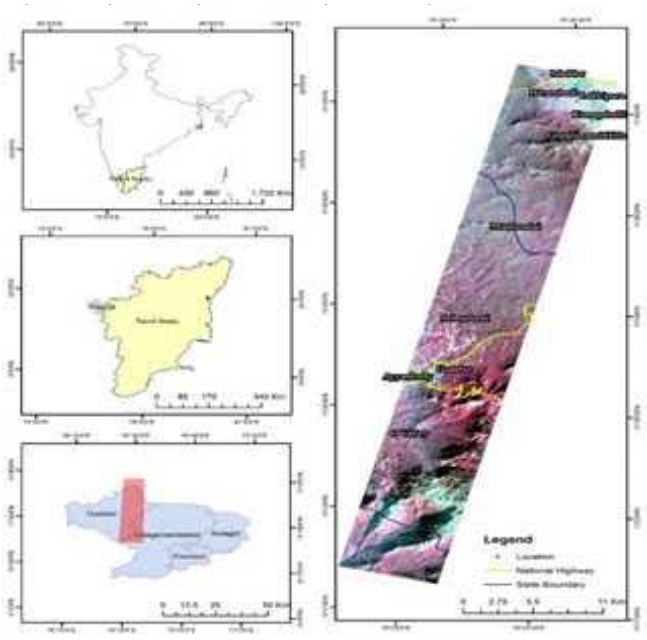

Figure 1. Map showing the study area (Mudumalai Tiger Reserve in the North and Nilgiri Hills in the South)

summer during March to mid-May with maximum temperature up to ~35æ%C, while winter during November to February with minimum temperature up to ~12æ%C. The rainy season consists of the southwest and northeast monsoon, during mid-May to October months with the gradient decreasing sharply from west to east.

DATA AND METHODOLOGY

In the present study, Sentinel 2A (acquired on 28 December 2016) and Hyperion satellite datasets (acquired on 18 December 2015) were used to map and compare forest composition through various indices (Fig. 2). Sentinel 2A is a high spatial resolution optical data at 10m with 12 spectral bands, while Hyperion is a hyperspectral sensor overboard on EO-1 that captures data at 30m spatial resolution and 10nm spectral resolution (Table 1). Considering the similar seasonality, meteorological and phenological conditions, the results of two different satellite data were compared.

Data Pre-Processing

The Hyperion imagery was atmospherically corrected using Fast Line-of-sight Atmospheric Analysis of Spectral Hypercubes (FLAASH) in the visible through near-infrared and short-wave infrared regions up to 3 ìm, employing first-principles atmospheric correction modelling tool for retrieving spectral reflectance (Fig. 3). In order to explain the relative contributions to the pixel radiance, a spatial average was performed through a spread function and later opted for removal of cloud pixels using a combination of brightness, band ratio, and water vapour tests (Matthew et al. 2000). The FLAASH module retrieves an estimated aerosol/ haze amount from selected dark land pixels in the scene (Kaufman et al. 1997) and FLAASH converts the radiance values to reflectance values (Fig. 4).

Vegetation Analysis

In order to identify various invasives, varied indices were performed using Sentinel 2A optical and Hyperion Hyperspectral satellite data. Normalized Difference Vegetation Index (NDVI), Anthocyanin Reflectance Index 1 (ARI-1), Carotenoid Reflectance Index 1 (CRI-1), Red edge NDVI (RENDVI), Enhanced Vegetation Index (EVI), Atmospherically Resistant Vegetation Index (ARVI), Vogelmann Red Edge Index1 (VERI-1), Modified Red edge NDVI (MRENDVI), Sum Green Index (SGI) were used to map the various pigment concentration of dominant

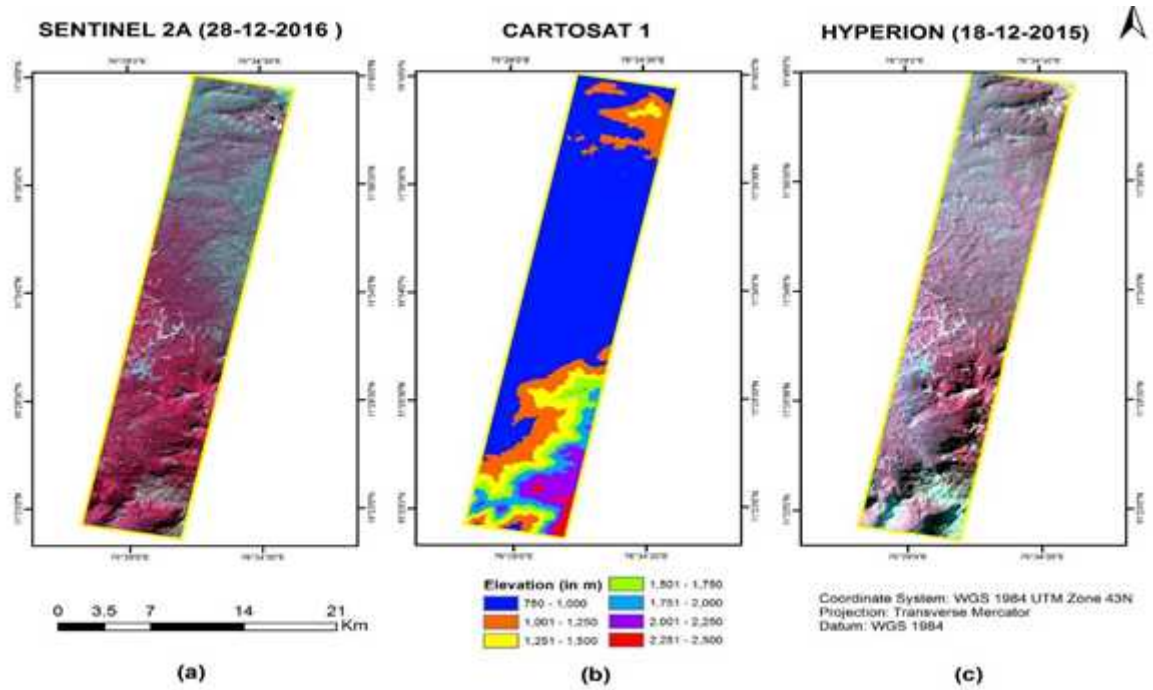

Figure 2. Map showing the different satellite imageries used in the study a) FCC of Sentinel 2A (RGB: 843), b) Elevation (in metres) and c) FCC of Hyperion (RGB: 52 30 20).

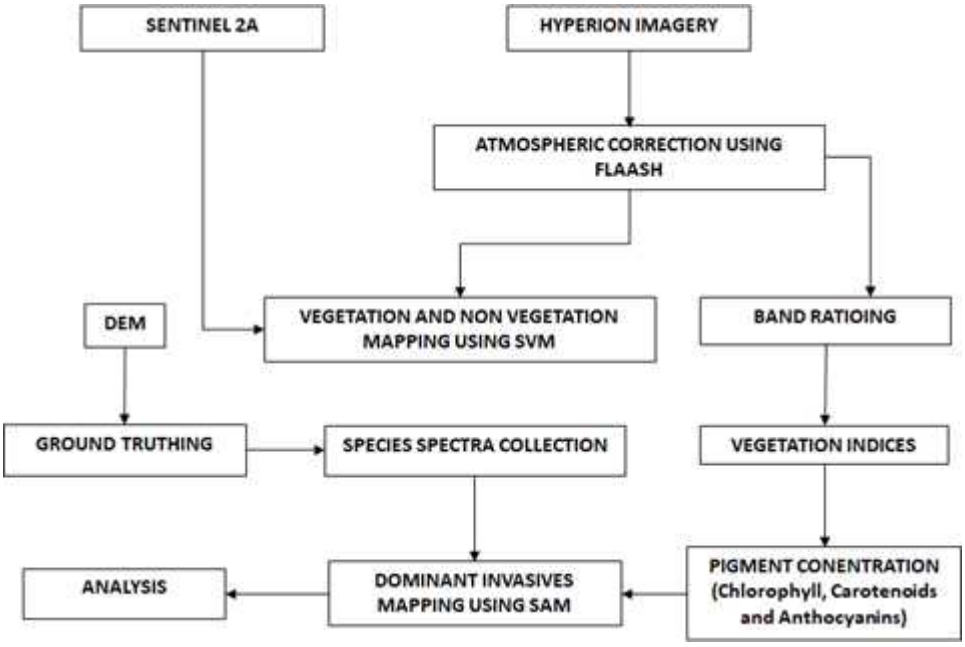

Figure 3. Methodology flow chart

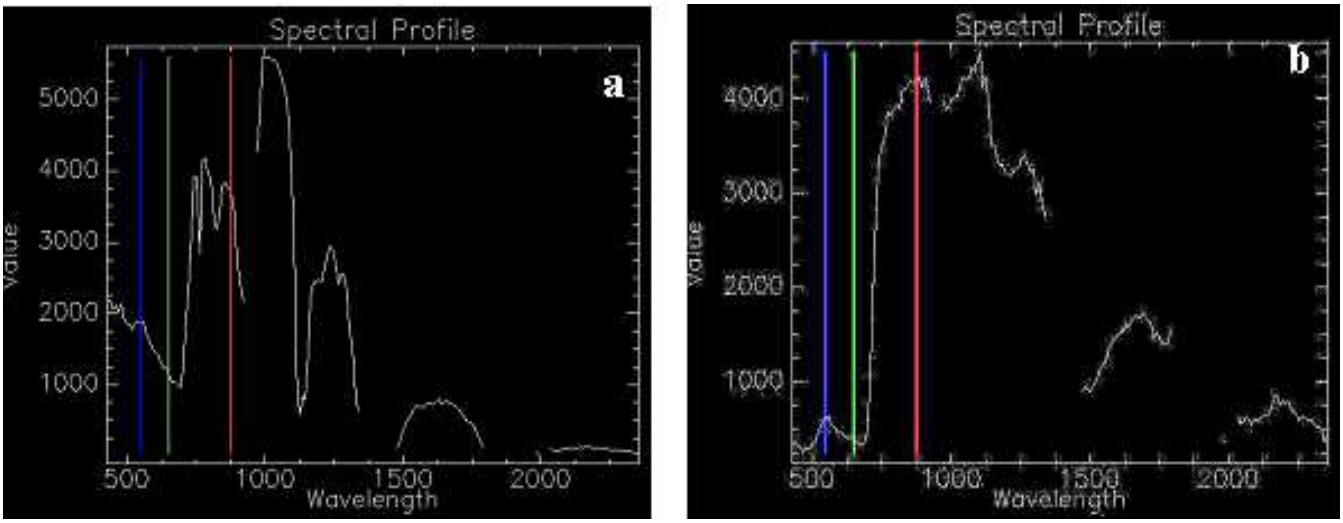

Figure 4. Spectra of vegetation (a) before atmospheric correction (b) after atmospheric correction using Hyperion satellite data.

Table 1. Satellite data used in the study

Sensor	Date of Acquisition	Path/ Row	Resolution			
			Spatial	Spectral	Radiometric	Temporal
Sentinel 2A	28-12-2016	11.26/76.41	10m	12	16 bit	10 days
Hyperion	18-12-2015	144/52	30m	220	12 bit	16 days
Cartosat 1	04-05-2015	-	30m	2	16 bit	126 days

Table 2. Vegetation indices adopted in the study

Acronym	Parameter	Wavelength sensitivity/ vegetation indices	Ref.
NDVI	Normalized Difference Vegetation Index	$\frac{\rho750 - \rho680}{\rho750 + \rho680}$	Rouse et al. 1974
ARI1	Anthocyanin Reflectance Index 1	$\frac{1}{\rho550} - \frac{1}{\rho700}$	Gitelson et al. 2001
CRI1	Carotenoid Reflectance Index 1	$\frac{1}{\rho510} - \frac{1}{\rho550}$	Gitelson et al. 2002
RENDVI	Red edge NDVI	$\frac{\rho750 - \rho705}{\rho750 + \rho705}$	Gitelson and Merzlyak 1994
EVI	Enhanced Vegetation Index	$2.5 * \frac{(NIR - Red)}{NIR + 6 * Red - 7.5 * Blue + 1}$	Huete et al. 2002
ARVI	Atmospherically Resistant Vegetation Index	$\frac{\rho800 - [\rho680 - \gamma(\rho450 - \rho680)]}{\rho800 + [\rho680 - \gamma(\rho450 - \rho680)]}$	Kaufman and Tanre 1992
VREI1	Vogelmann Red Edge Index1	$\frac{\rho740}{\rho720}$	Vogelmann and Moss 1993
MRENDVI	Modified Red edge NDVI	$\frac{\rho750 - \rho705}{\rho750 + \rho705 - 2 * \rho445}$	Datt 1999
SGI	Sum Green Index	Mean of reflectance across the 500 nm to 600 nm portion of the spectrum	Lobell and Asner 2003

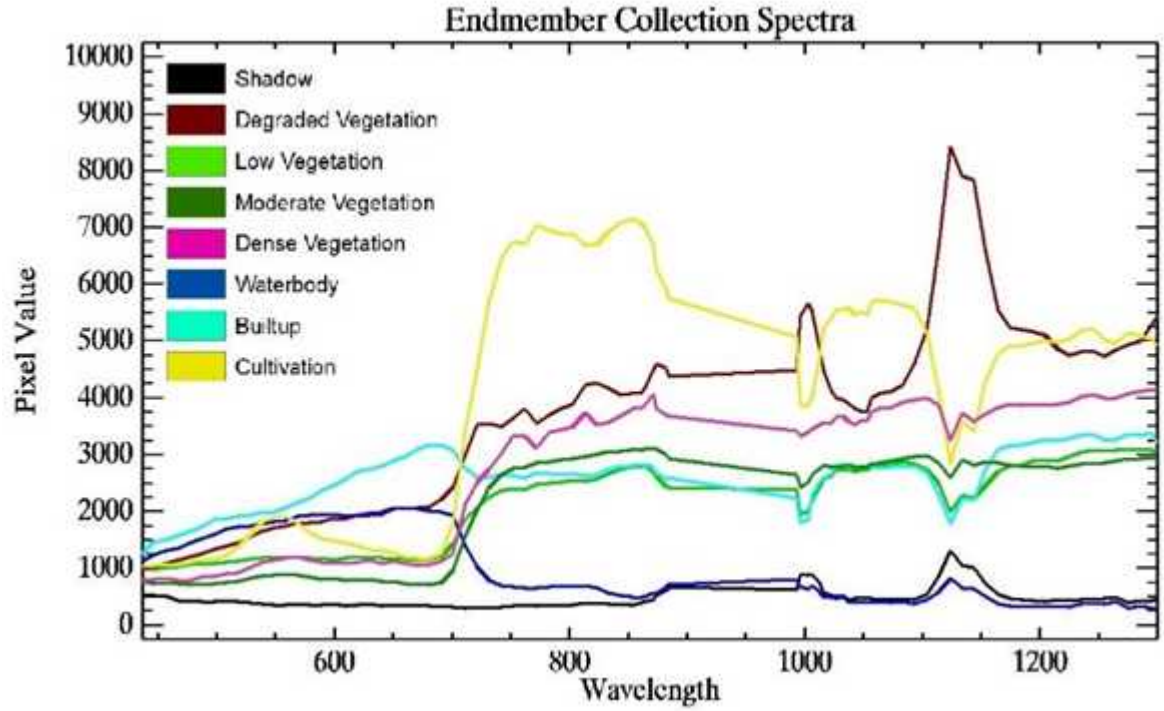

Figure 5(a). Endmember spectra collection of different classes

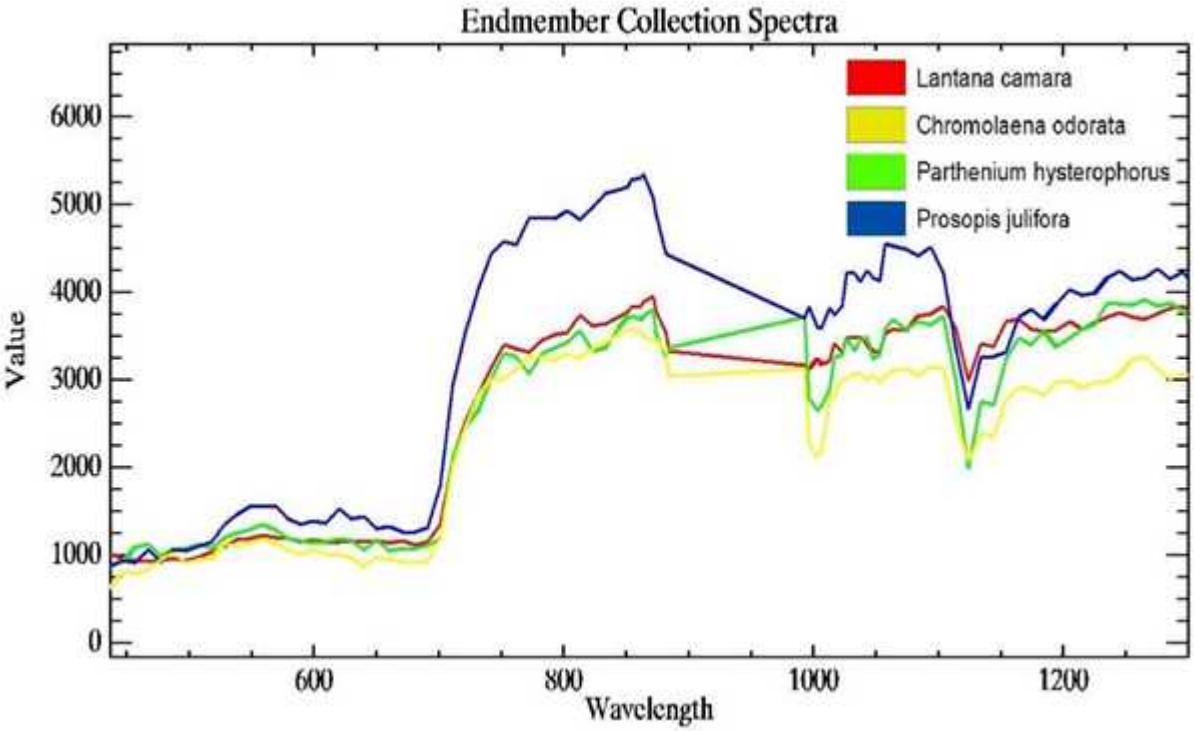

Figure 5(b). Endmember spectra collection of different species

invasives in MTR (Table 2).

A pixel-based supervised classification was performed using SVM in ENVI version 5.2, which is a supervised machine learning technique that categorises data on the basis of a sophisticated statistical analysis considering an optimum separation hyperplane with a set of training data. Recent studies have reported that SVMs are one of the best classification methods for robust datasets like Hyperion (Petropoulos et al. 2012, Elatawneh et al. 2014, Lamine et al. 2018, Lin and Zhang 2020). Training sites representative of each of the classes

were collected from the Hyperion imagery based on ground-truthing. The spectra of all classes had been generated using the (ROI) tool (Fig. 5a). The maximum value (i.e., 100) was set to the penalty parameter which required all pixels to be allocated to one specific class. In order to analyse the image of Hyperion with full resolution, the zero value is set to the pyramid parameter. The probability classification limit is set to a null value in order to assign the whole pixel to a certain class, leaving no pixels unclassified in the picture. Later, the endmember spectra of dominant invasives is extracted from the hyperion image with the help of ground truthing (Fig. 5b). This spectra was incorporated in SAM based classification by determining the angle between reference spectra and image spectra treating them as vectors in an n-dimensional space. A mean value of 0.5 radian angle was selected for discrimination of classes.

RESULTS

Analysing Vegetation Vigour and Pigmentation in Mudumalai Tiger Reserve

Normalised Difference Vegetation Index

The NDVI of Sentinel 2A was evaluated using the near infra-red (785-899 nm) and green (543-578 nm) bands. It has been observed that the NDVI values in the MTR range from -0.36 to 0.9 (Fig. 6a). The majority of the study area exhibited positive NDVI implying the existence of vegetation, in contrast to negative NDVI values in very few parts. The north-eastern part of the MTR has low positive NDVI values (0.1 to 0.3) implying low vegetation cover, followed by the north-western parts with moderate NDVI values (0.3 to 0.5) exhibiting moderate vegetation cover, while the central region with high NDVI values (0.5 to 0.8) signifying dense vegetation cover. The NDVI of Hyperion was evaluated using the 48th (834 nm) and 33rd (681 nm) spectral bands, in which the NDVI values range from -0.7 to 0.78 in MTR (Fig. 6b). The majority of the area of MTR has positive NDVI values (0.5 to 06) implying moderate vegetation, while the northern part has moderate NDVI values (0.4 to 0.5), in contrast, a very few parts have negative NDVI values implying the existence of waterbody, built up, and shadow (Fig.

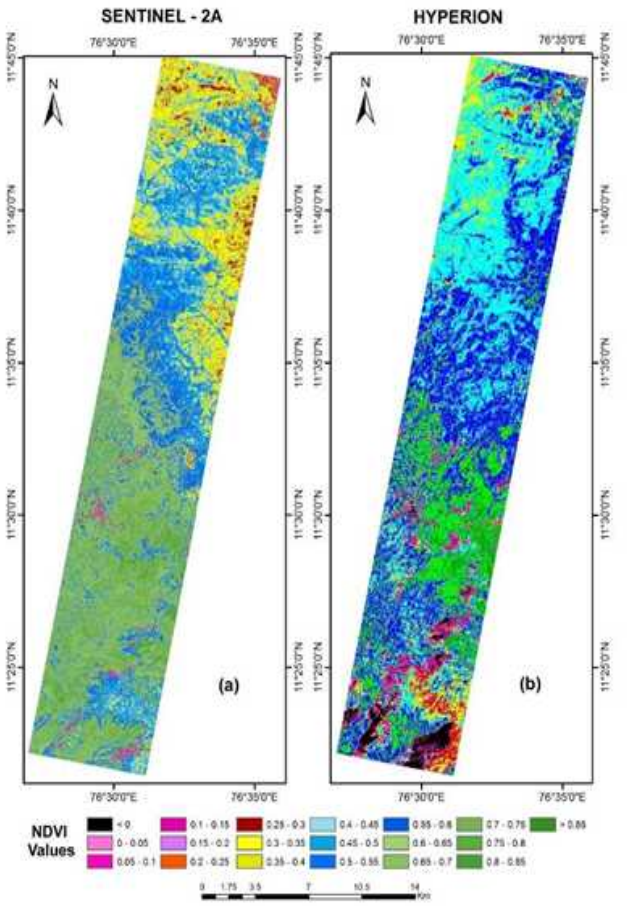

Figure 6. Comparing NDVI of parts of Mudumalai Tiger Reserve based on (a) Sentinel 2A (acquired on 28 December 2016), and (b) Hyperion data (18 December 2015)

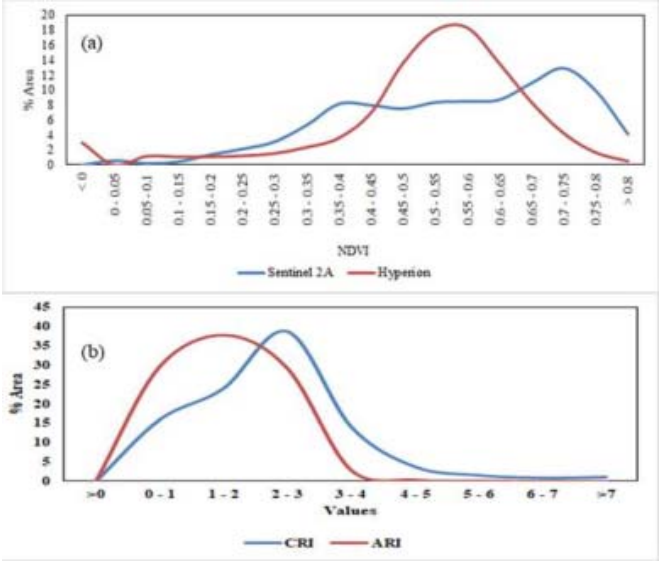

Figure 7. Comparison of (a) NDVI values based on Sentinel 2A and Hyperion data, and (b) carotenoid reflectance index and anthocyanin reflectance index in Mudumalai Tiger Reserve

7a).

Carotenoid Reflectance Index

The carotenoid reflectance index was used to evaluate the concentration of carotenoid in the forest vegetation in MTR using the 16th (508 nm) and 20th (549 nm) band of Hyperion data. The CRI values are ranging from -0.7 to 6.4, having a majority of low CRI values (1 to 3). The moderate CRI (2 to 3) was observed in the southern parts while the low CRI (1 to 2) was recorded in northern parts (Figs. 7b and 8). A very few parts have negative CRI values implying the non-vegetative features.

Anthocyanin Reflectance Index

The anthocyanin reflectance index was analysed using the 20th (549 nm) and 35th (701 nm) bands of Hyperion satellite data. The ARI values are ranging from -0.6 to 4.5 in the MTR, having dominance of moderately low CRI (0.1 to 2). The moderate ARI (1 to 2) was observed in the southern parts while the low ARI (> 1) was recorded in northern parts (Figs. 7b and 8).

Other Vegetation Indices

The red edge normalised difference vegetation index was evaluated using 35th (702 nm) and 40th (752 nm) bands of Hyperion satellite data. The RENDVI values are ranging from -0.70 to 0.73 in the MTR (Figs. 9a and 10a), with a dominance of low RENDVI (0.1 to 0.2). The very high RENDVI (>0.6) was observed in the northern parts while the moderate RENDVI (<0.2) was recorded in southern parts of MTR. The enhanced vegetation index was evaluated using NIR (800 nm), red (680 nm) and blue (450 nm) bands of Hyperion satellite data in MTR. The EVI values are ranging from -0.5 to 0.94 (Figs. 9b and 10a), with a dominance of moderately high EVI (0.4 to 0.6). The moderate EVI (0.4-0.5) was observed in the southern parts, while the low EVI (0.2-0.4) was recorded in the northern parts of MTR. The sum green index was evaluated using the mean of 15 to 25 (500-600 nm) bands of Hyperion satellite data. The SGI values are ranging from -0.7 to 0.24 (Figs. 9c and 10b), with a dominance of moderately high SGI (0.1 to 0.15). The moderate SGI (0.05-0.15) was observed in the northern parts, while the low SGI (<0.1) was recorded in the southern parts of MTR. The atmospheric resistant vegetation index was evaluated using NIR (800 nm), red (680 nm) and blue (450 nm) bands of Hyperion satellite data. The ARVI values are ranging from -0.46 to 0.98 in the study area (Figs. 9d and 10a), with a dominance of moderate ARVI (0.3 to 0.5). The moderate ARVI (0.3 to 0.4) was observed in the northern parts, while the low ARVI (0.3 to 0.4) was recorded in the southern parts of MTR. The Vogelmann red edge index was evaluated using the 37th (722 nm) and 39th (742 nm) band of Hyperion satellite data.

The VREI values are ranging from -0.73 to 1.98 (Figs. 9e and 10c), with a dominance of high VREI (1 to 2). The moderately low VREI (1 to 1.5) was observed in the northern parts, while the high VREI (> 1.5) was recorded in southern parts of MTR. The modified red edge normalised difference vegetation index was evaluated using 10th (447 nm), 35th (702 nm), and 40th (752 nm) bands of Hyperion data. The MRENDVI values are ranging from -0.87 to 0.96 (Figure 9f &10a), with a dominance of moderate and high MRENDVI (0.1 to 0.5). The moderate MRENDVI (0.1 to 0.43) was observed in the northern parts, while the low MRENDVI (<0.1) was recorded in southern parts of MTR (Table 4).

Forest Cover Classification and Invasion

The forest area of MTR was classified based on density classes, employing machine learning SVM algorithms using Hyperion and Sentinel 2A satellite data (Fig. 11 and Table 5). The study exhibited a large area under forest cover as classified using Sentinel 2A (95.65%), and Hyperion satellite data (84.16%). The majority of the forest area was classified as dense forest (30.15%-Sentinel 2A, 40.64%-Hyperion), followed by Moderate dense forest (22.04%-Sentinel 2A, 27.81%-Hyperion), low density forest (33.44%-Sentinel 2A, 15.71%-Hyperion), and degraded forest (10.02%-Sentinel 2A, 6.48%-Hyperion). In contrast, the non-forest cover comprising cultivated land (2.70%-Sentinel 2A, 0.49%-Hyperion), Built-Up (0.49% - Sentinel 2A, 0.07%-Hyperion), Waterbody, and others (1.16%-Sentinel 2A, 8.75%-Hyperion).

The composition of dominant forest cover was evaluated using different invasive species including, *Lantana camara, Parthenium hysterophorus, Prosopis juliflora,* and *Chromolaena odorata* based on field observation in MTR. The study exhibited the dominance of *L. camara* in the northern, southern and central parts followed by *C. odorata* in the neighborhood of *L. camara* in northern and central

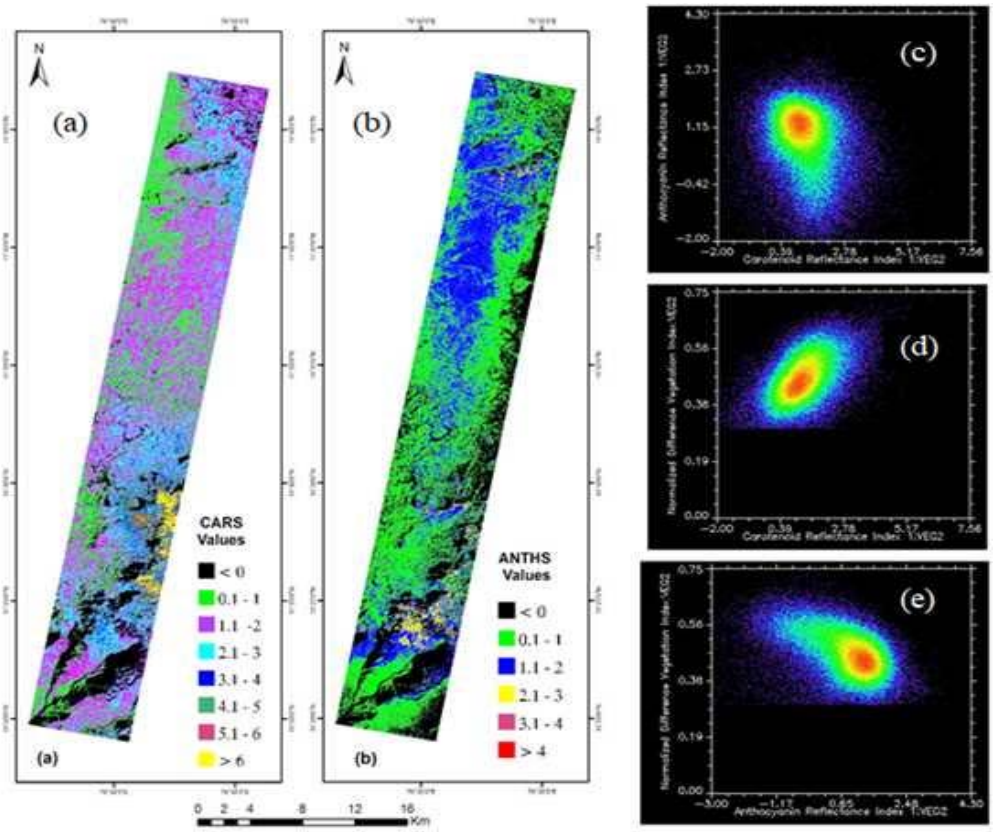

Figure 8. Hyperion satellite data-based (a) carotenoid reflectance index (b) anthocyanin reflectance index of parts of MTR, and scatter plots of (c) NDVI *vs* ARI, (d) CRI *vs* ARI, and (e) CRI *vs* NDVI.

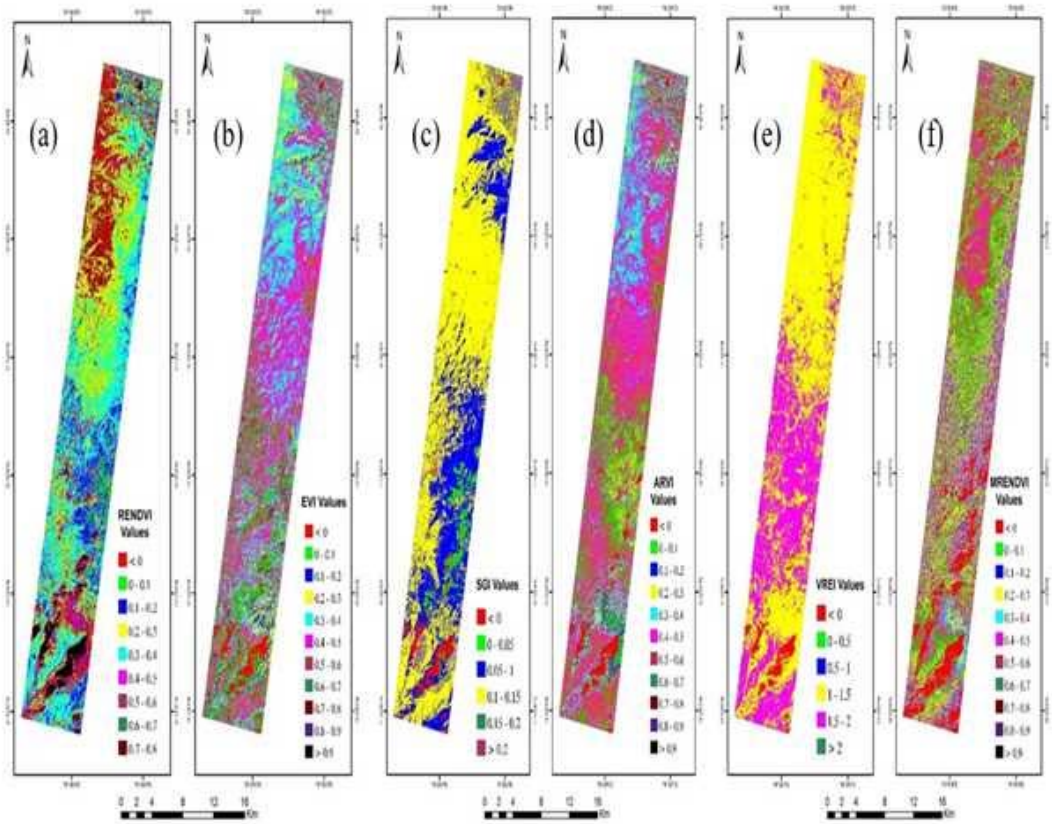

Figure 9. Hyperion satellite data-based (a) Red edge normalised difference vegetation index, (b) enhanced vegetation index, (c) sum green index, (d) atmospherically resistant vegetation index, (e) Vogelmann red edge index, (f) modified red edge normalized difference vegetation index of Mudumalai Tiger Reserve

Table 4. Statistics of RENDVI, EVI, SGI, ARVI, VREI, and MRENDVI based on Hyperion satellite data in Mudumalai Tiger Reserve

Values	Percent	Area (in Km²)	Values	Percent	Area (in Km²)
a. Red Edge Normalised Difference Vegetation Index (RENDVI)			**d. Atmospherically resistant vegetation index (ARVI)**		
< 0	3.57	13.97	< 0	4.66	18.21
0 - 0.1	2.34	9.13	0 - 0.1	2.09	8.15
0.1 - 0.2	4.11	16.06	0.1 - 0.2	3.58	13.98
0.2 - 0.3	17.30	67.63	0.2 - 0.3	6.04	23.60
0.3 - 0.4	31.67	123.76	0.3 - 0.4	15.93	62.28
0.4 - 0.5	28.29	110.55	0.4 - 0.5	25.99	101.58
0.5 - 0.6	11.00	43.01	0.5 - 0.6	25.19	98.44
0.6 - 0.7	1.69	6.60	0.6 - 0.7	12.10	47.29
> 0.7	0.03	0.12	0.7 - 0.8	3.62	14.16
b. Enhanced Vegetation Index (EVI)			0.8 - 0.9	0.63	2.45
< 0	2.94	11.49	> 0.9	0.18	0.71
0 - 0.1	4.83	18.86	**e. Vogelmann red edge index (VREI)**		
0.1 - 0.2	4.97	19.43	< 0	0.00	0.00
0.2 - 0.3	11.11	43.42	0 - 0.5	2.93	11.46
0.3 - 0.4	26.06	101.86	0.5 - 1	0.01	0.06
0.4 - 0.5	26.33	102.91	1 - 1.5	0.42	1.65
0.5 - 0.6	14.03	54.84	1.5 - 2	62.90	245.83
0.6 - 0.7	6.55	25.58	2 - 2.5	33.47	130.82
0.7 - 0.8	2.42	9.47	> 2.5	0.26	1.03
0.8 - 0.9	0.63	2.47	**f. Modified red edge normalized difference vegetation index (MRENDVI)**		
> 0.9	0.13	0.51	< 0	12.94	50.59
c. Sum green index (SGI)			0 - 0.1	0.56	2.19
< 0	0.01	0.03	0.1 - 0.2	0.67	2.62
0 - 0.05	2.93	11.46	0.2 - 0.3	1.48	5.77
0.05 - 0.1	3.06	11.94	0.3 - 0.4	2.92	11.40
0.1 - 0.15	29.39	114.85	0.4 - 0.5	6.55	25.59
0.15 - 0.2	56.76	221.83	0.5 - 0.6	14.11	55.16
> 0.2	7.53	29.45	0.6 - 0.7	19.46	76.04
			0.7 - 0.8	20.91	81.71
			0.8 - 0.9	14.10	55.10
			> 0.9	6.31	24.67

Table 5. Statistics of different classes of Sentinel 2A and Hyperion data

Class Name	Sentinel 2A		Hyperion	
	Percent	Area (in Km²)	Percent	Area (in Km²)
Dense Forest	30.15	100.00	40.64	130.86
Moderate dense Forest	22.04	73.10	27.81	89.54
Low density Forest	33.44	110.92	15.71	50.60
Degraded Forest	10.02	33.25	6.48	20.88
Non-Forest	4.36	14.46	9.33	30.08

parts, while *P. juliflora* in central, *P. hysterophorus* in central to northern parts in a scattered manner. The vegetation vigour and pigment concentration exhibited moderate to high NDVI (0.4 to 0.65) of *L. camara,* with moderate CRI (0 to 0.4) and low ARI (0 to 0.2). While, *P. hysterophorus* had moderate to

Table 6. NDVI, CRI, and ARI values of different invasives in low, medium, and high classes (LC - *Lantana camara;* PH - *Parthenium hysterophorus;* PJ - *Prosopis juliflora;* CO - *Chromolaena odorata*)

	Values	LC	PH	PJ	CO
NDVI					
Low	< 0	0	0	0	0
	0 - 0.05	0	0	0	0
	0.05 - 0.1	0	0	0	0
	0.1 - 0.15	0	0	0	0
	0.15 - 0.2	0	0	0	0
	0.2 - 0.25	0	0	0	0
Moderate	0.25 - 0.3	0	0	0	0
	0.3 - 0.35	0	0	0	0
	0.35 - 0.4	1	2	0	1
	0.4 - 0.45	21	5	6	30
	0.45 - 0.5	71	44	37	256
High	0.5 - 0.55	59	45	103	1005
	0.55 - 0.6	63	28	209	1183
	0.6 - 0.65	29	6	138	783
	0.65 - 0.7	4	0	61	227
	0.7 - 0.75	0	0	12	11
	> 0.75	0	0	2	0
	Total	248	130	568	3496
CRI					
Low	< 0	0	1	0	26
	0 - 0.1	30	32	18	526
	0.1 - 0.2	134	84	209	1761
Moderate	0.2 - 0.3	69	13	298	1066
	0.3 - 0.4	13	0	39	107
High	0.4 - 0.5	2	0	4	10
	0.5 - 0.6	0	0	0	0
	> 0.6	0	0	0	0
	Total	248	130	568	3496
ARI					
Low	< 0	24	30	85	927
	0 - 0.1	127	66	392	2018
Moderate	0.1 - 0.2	96	34	89	543
	0.2 - 0.3	1	0	2	8
High	0.3 - 0.4	0	0	0	0
	> 0.4	0	0	0	0
	Total	248	130	568	3496

Table 7. NDVI, CRI, and ARI range of dominant invasives

Species	NDVI	CRI	ARI
Lantana camara	0.4 - 0.65	0 - 0.4	< 0 - 0.2
Parthenium hysterophorus	0.45 - 0.6	0 - 0.3	< 0 - 0.2
Prosopis juliflora	0.45 - 0.75	0 - 0.4	< 0 - 0.2
Chromolaena odorata	0.4 - 0.7	< 0 - 0.5	< 0 - 0.3

high NDVI (0.45 to 0.6), low CRI (0 to 0.3), and low ARI (< 0 to 0.2); *P. juliflora* had moderate to very high NDVI (0.45 to 0.75), moderate CRI (0 to 0.4), and low ARI (< 0 to 0.2); and *C. odorata* had moderate to very high NDVI (0.4 to 0.7), moderate CRI (0 to 0.5), and low ARI (< 0 to 0.3) in major parts of MTR (Tables 6 and 7).

DISCUSSION

The comparative assessment of NDVI based on Sentinel 2A and Hyperion satellite data exhibited a difference in the values of NDVI that depicts the sensitivity of different spectral bands in measuring the vegetation vigour. The narrow bands in Hyperion satellite data were providing more precise information in terms of forest composition, its pigment concentration, and traits. Similar findings with good agreement between the Hyperion and the Sentinel-2A data, with a slight overestimation in NDVI as measured using Sentinel-2A compared to the hyperspectral mosaic as reported in an open-canopy coniferous forest of Spain (Zarco-Tejada et al. 2019). The discrepancies may be attributed to sensor noise, erroneous spatial co-registration, and variation in spectral channels (Zarco-Tejada et al. 2019). The unique and narrower band composition of hyperion satellite data exhibited low CRI values (1 to 3) in the majority of MTR in contrast to moderately low ARI (0.1 to 2), which signifies the majority of forest has good health (Kayet et al. 2019). While the other indices demonstrated the high MRENDVI, moderate ARVI, moderately low EVI and RENDVI in major parts of MTR.

The comparative assessment of highlights the improved results of hyperion based forest cover density compared to Sentinel 2A and with dominance of dense forest (40.64% - Hyperion), followed by moderate dense forest (22.04% - Sentinel 2A, 27.81% - Hyperion) in MTR and the large parts of the MTR were invaded by *L. camara, P. hysterophorus, P. juliflora,* and *C. odorata* in MTR. *L. camara* and *C. odorata* were mainly found in the MTR situated in the northern part of study area, whereas *P. juliflora* and *P. hysterophorus* were found nearby the built up area across roads situated in the central parts in MTR. The vegetation vigour and pigment concentration exhibited the moderate to high

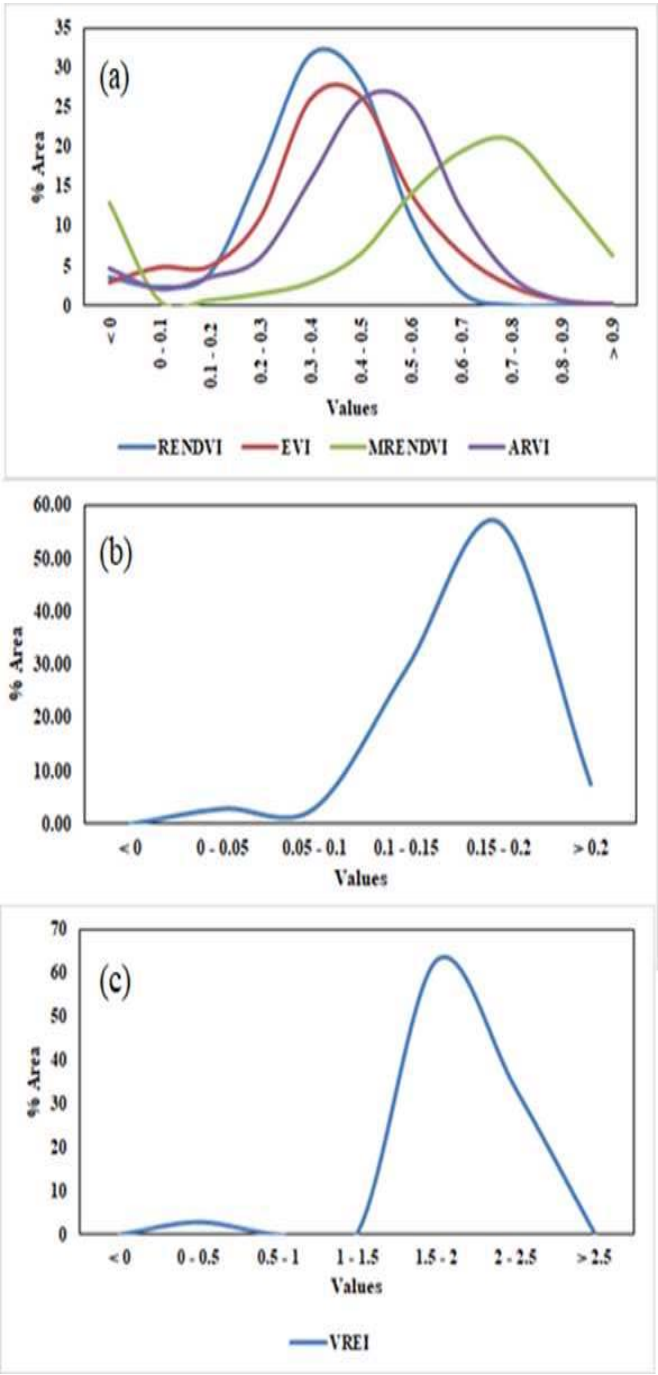

Figure 10. Graphical representation of area coverage of indices under different classes (a) RENDVI, EVI, MRENDVI, ARVI, (b) SGI, and (c) VREI

NDVI and low to moderate CRI and ARI of invasives that may be useful in mapping the characteristics of invasives that aid in devising proper forest management plans.

In conformity with the present study, SVM performed with utmost accuracy in the comparative study of decision makers, SVMs, and maximum probability classifiers (Otuke and Blaschk 2010).

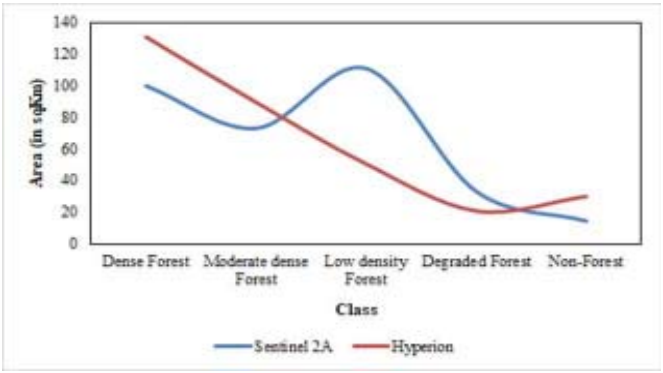

Figure 11. Comparative assessment of forest density in MTR based on Hyperion and Sentinel 2A satellite data

The Hyperion and Landsat TM sensors were used for discrimination and classification of broadleaved evergreen and conifer forest tree species in West Himalaya and SVM produced a better species classification (overall accuracy 82.27%, kappa statistic 0.79) than SAM (overall accuracy 74.68%, kappa statistic 0.70) (George et al. 2014). Similarly, the effectiveness of SVM and ANN classifiers for hyperspectral image classification over an agriculture area was assessed using data from an aerial hyperspectral sensing system, results exhibited SVM method has very low misclassification rates, as compared to the ANN approach (Karimi et al. 2006). SVM classifiers required less training time and fewer parameters compared to other classifiers (Dixon and Candede 2008), which can effectively be used directly for processed Hyperion data without dimensionality reduction (Vyas et al. 2011). The unique band availability in Hyperion satellite data enables to map the specific properties of vegetation, which are underestimated by the multispectral satellite images.

The spectral resolution had some noticeable influences in mapping of the major invasive species as Hyperion with 242 bands gives a better understanding of spectral response of the features in the whole spectrum compared to Sentinel 2A having 13 bands in VIS and NIR portions of the spectrum. The Hyperion data was acquired one year before the acquisition of Sentinel 2A data that may induce minor differences including cultivation, due to crop rotation and yearly precipitation fluctuations.

The successful use of hyperspectral data for detecting and mapping species needs careful

consideration of hyperspectral sensors/systems, imaging pre-translation methods, type and properties of vegetation, phonological change and environmental context before a project starts. This has a substantial influence on the success of remote sensors and mapping species due to temporal, geographical, radiometric, and spectral resolutions of hyper-spectral data.

CONCLUSION

The hyperspectral system's potential contribution is its capacity to provide novel indices that include wavelengths not captured in any broadband system and measure absorptions that are special to significant bio-chemical and/or biophysical vegetation levels. The large parts of MTR is having high NDVI exhibiting good vegetation vigour, while moderate CRI and low ARI reflected the foliar pigment concentration. A large part of MTR is dominated by dense forest (40.64%-Hyperion), a major part of it was invaded by *L. camara* and *C. odorata*. The study highlights finer mapping of species through hyperspectral remote sensing in conjugation with detailed field observations that may be useful in devising effective forest management plans. Hyperion hyperspectral satellite data enables effectively as compared to multispectral imaging (Sentinel 2A) and evolved as advantageous tools for vegetation monitoring, producing foliar pigment maps that will enhance our understanding of photosynthetic status, physiological condition, and detection of forest degradation and upgradation over time.

ACKNOWLEDGEMENTS

The authors are thankful to Copernicus and USGS for providing a satellite data repository of Hyperion and Sentinel 2A freely. The authors are grateful to Space Application Centre, Indian Space Research Organization (ISRO), Government of India for the funding provided under Airborne Visible/Infrared Imaging Spectrometer Next Generation AO project (EPSA/4.20/2017-Site 60). The authors sincerely acknowledge the State Forest Department, Government of Tamil Nadu for their support in the field data collection, especially Shri A. Udhayan, Indian Forest Service (IFS), APCCF (Bio-Con) for extending continuous support throughout ground truth and field validation.

Conflict of interest: The authors declare no conflict of interest

Authors' contribution: All authors contributed equally

REFERENCES

Aneece, I. and Thenkabail, P. 2018. Accuracies achieved in classifying five leading world crop types and their growth stages using optimal earth observing-1 hyperion hyperspectral narrow bands on google earth engine. Remote Sensing, 10(12), 2027.

Arockraj. S., Kumar, A., Hoda, N. and Jeyaseelan, A.T. 2015. Quantification and identification of tree species in open mixed forests using high resolution QuickBird satellite imagery. Journal of Tropical Forestry and Environment, 5(2), 40-53.

Ashokkumar, L. and Shanmugam, S. 2014. Hyperspectral band selection and classification of Hyperion image of Bhitarkanika mangrove ecosystem, eastern India. In: Remote Sensing for Agriculture, Ecosystems, and Hydrology XVI, 9239, 923914, International Society for Optics and Photonics.

Asner, G.P. and Vitousek, P.M. 2005. Remote analysis of biological invasion and biogeochemical change. Proceedings of the National Academy of Sciences 102, 4383e4386.

Asner, G.P., Jones, M.O., Martin, R.E., Knapp, D.E. and Hughes, R.F. 2008. Remote sensing of native and invasive species in Hawaiian forests. Remote Sensing of Environment, 112(5), 1912–1926.

Barker, D.H., Seaton, G.G.R. and Robinson, S.A. 1997. Internal and external photoprotection in developing leaves of the CAM plant *Cotyledon orbiculata*. Plant, Cell & Environment, 20(5), 617–624.

Bartley, G.E. and Scolnik, P.A. 1995. Plant carotenoids: pigments for photoprotection, visual attraction, and human health. The Plant Cell, 7(7), 1027.

Chambers, J.Q., Asner, G.P., Morton, D.C., Anderson, L.O., Saatchi, S.S., Espírito-Santo, F.D., Palace, M. and Souza Jr, C. 2007. Regional ecosystem structure and function: ecological insights from remote sensing of tropical forests. Trends in Ecology and Evolution, 22(8), 414–423.

Chazdon, R. L. 2003. Tropical forest recovery: legacies of human impact and natural disturbances. Perspectives in Plant Ecology, Evolution and Systematics, 6(1-2), 51–71.

Chutia, D., Borah, N., Baruah, D., Bhattacharyya, D.K., Raju, P.L.N. and Sarma, K.K. 2020. An effective approach for improving the accuracy of a random forest classifier in the classification of Hyperion data. Applied Geomatics, 12(1), 95-105.

Close, D.C. and Beadle, C.L. 2003. The ecophysiology of foliar anthocyanin. The Botanical Review, 69(2), 149–161.

Czech, B. and Krausman, P.R. 1997. Distribution and causation of species endangerment in the United States. Science, 277(5329), 1116–1117.

Dao, P.D., Axiotis, A. and He, Y. 2021. Mapping native and invasive grassland species and characterizing topography-driven species dynamics using high spatial resolution hyperspectral imagery. International Journal of Applied Earth Observation and Geoinformation, 104, 102542.

Datt, B. 1999. A new reflectance index for remote sensing of chlorophyll content in higher plants: tests using Eucalyptus leaves. Journal of Plant Physiology, 154(1), 30-36.

Dawson, T.P., North, P.R.J., Plummer, S.E. and Curran, P.J. 2003. Forest ecosystem chlorophyll content: implications for remotely sensed estimates of net primary productivity. International Journal of Remote Sensing, 24(3), 611–617.

Dewey, S.A., Price, K.P. and Ramsey, D. 1991. Satellite remote sensing to predict potential distribution of dyers woad (*Isatis tinctoria*). Weed Technology, 5(3), 479–484.

Dixon, B. and Candade, N. 2008. Multispectral land use classification using neural networks and support vector machines: one or the other, or both? International Journal of Remote Sensing, 29(4), 1185-1206.

Edge, R., McGarvey, D.J. and Truscott, T.G. 1997. The carotenoids as antioxidants-a review. Journal of Photochemistry and Photobiology B: Biology, 41, 189–200.

Elatawneh, A., Kalaitzidis, C., Petropoulos, G. P. and Schneider, T. 2014. Evaluation of diverse classification approaches for land use/cover mapping in a Mediterranean region utilizing Hyperion data. International Journal of Digital Earth, 7(3), 194-216.

Filella, I., Serrano, L., Serra, J. and Penuelas, J. 1995. Evaluating wheat nitrogen status with canopy reflectance indices and discriminant analysis. Crop Science, 35(5), 1400–1405.

George, R., Padalia, H., & Kushwaha, S. P. S. 2014. Forest tree species discrimination in western Himalaya using EO-1 Hyperion. International Journal of Applied Earth Observation and Geoinformation, 28, 140-149.

Gitelson, A.A., Merzlyak, M.N. and Chivkunova, O.B. 2001. Optical properties and nondestructive estimation of anthocyanin content in plant leaves. Photochemistry and Photobiology, 74(1), 38-45.

Gitelson, A.A., Zur, Y., Chivkunova, O.B. and Merzlyak, M. N. 2002. Assessing carotenoid content in plant leaves with reflectance spectroscopy. Photochemistry and Photobiology, 75(3), 272-281.

Gitelson, A. and Merzlyak, M.N. 1994. Spectral reflectance changes associated with autumn senescence of *Aesculus hippocastanum* L. and *Acer platanoides* L. leaves. Spectral features and relation to chlorophyll estimation. Journal of Plant Physiology, 143(3), 286-292.

Gould, K., Davies, K.M. and Winefield, C. 2008. Anthocyanins: biosynthesis, functions, and applications. Springer Science & Business Media.

Huete, A., Didan, K., Miura, T., Rodriguez, E.P., Gao, X. and Ferreira, L.G. 2002. Overview of the radiometric and biophysical performance of the MODIS vegetation indices. Remote Sensing of Environment, 83(1-2), 195-213.

Karimi, Y., Prasher, S.O., Patel, R.M. and Kim, S.H. 2006. Application of support vector machine technology for weed and nitrogen stress detection in corn. Computers and Electronics in Agriculture, 51(1-2), 99-109.

Kaufman, Y.J. and Tanre, D. 1992. Atmospherically resistant vegetation index (ARVI) for EOS-MODIS. IEEE transactions on Geoscience and Remote Sensing, 30(2), 261-270.

Kaufman, Y.J., Wald, A.E., Remer, L.A., Gao, B.-C., Li, R.-R. and Flynn, L. 1997. The MODIS 2.1-/spl mu/m channel-correlation with visible reflectance for use in remote sensing of aerosol. IEEE transactions on Geoscience and Remote Sensing, 35(5), 1286–1298.

Kayet, N., Pathak, K., Chakrabarty, A., Singh, C.P., Chowdary, V.M., Kumar, S. and Sahoo, S. 2019. Forest health assessment for geo-environmental planning and management in hilltop mining areas using Hyperion and Landsat data. Ecological Indicators, 106, 105471.

Kishore, B.S.P.C., Kumar, A., Lele, N., Srivastava, P., Saikia, P., Pandey, A.C., Bhattacharya, B. and Khan, M.L. 2020. Major forests and plant species discrimination in Mudumalai forest region using airborne hyperspectral sensing. Journal of Asia Pacific Biodiversity, 13(4), 637-651.

Kokaly, R.F., Despain, D.G., Clark, R.N. and Livo, K.E. 2003. Mapping vegetation in Yellowstone National Park using spectral feature analysis of AVIRIS data. Remote Sensing of Environment, 84(3), 437-456.

Kothandaraman, S., Dar, J.A., Sundarapandian, S., Dayanandan, S. and Khan, M.L. 2020. Ecosystem-level carbon storage and its links to diversity, structural and environmental drivers in tropical forests of Western Ghats. Scientific Reports, 10(1), 13444.

Kumar, R. and Saikia, P. 2020. Forests resources of Jharkhand, Eastern India: Socio-economic and bioecological perspectives. pp. 61-101. In: Roy, N., Roychoudhury, S., Nautiyal, S., Agarwal, S.K. and Baksi, S. (Eds.), Socio-economic and Eco-Biological Dimensions in Resource use and Conservation - Strategies for Sustainability, Springer International Publishing, Switzerland, .

Lamine, S., Petropoulos, G.P., Singh, S.K., Szabó, S., Bachari, N.E.I., Srivastava, P.K. and Suman, S. 2018. Quantifying land use/land cover spatio-temporal landscape pattern dynamics from Hyperion using SVMs classifier and FRAGSTATS®. Geocarto International, 33(8), 862-878.

Lawrence, R.L., Wood, S.D. and Sheley, R.L. 2006. Mapping invasive plants using hyperspectral imagery and Breiman Cutler classifications (RandomForest). Remote Sensing of Environment, 100(3), 356-362.

Lin, Z. and Zhang, G. 2020. Genetic algorithm-based parameter optimization for EO-1 Hyperion remote sensing image classification. European Journal of Remote Sensing, 53(1), 124-131.

Lobell, D. and Asner, G. 2004. Hyperion studies of crop stress in Mexico. In Proceedings of the 12 Annual JPL Airborne

Earth Science Workshop, Pasadena, CA, USA, 24–28.

Matthew, M.W., Adler-Golden, S.M., Berk, A., Richtsmeier, S.C., Levine, R.Y., Bernstein, L.S., Acharya, P.K., Anderson, G.P., Felde, G.W. and Hoke, M.L. 2000. Status of atmospheric correction using a MODTRAN4-based algorithm, in: Algorithms for Multispectral, Hyperspectral, and Ultraspectral Imagery VI. International Society for Optics and Photonics, pp. 199–207.

Moran, J. A., Mitchell, A.K., Goodmanson, G. and Stockburger, K. A. 2000. Differentiation among effects of nitrogen fertilization treatments on conifer seedlings by foliar reflectance: a comparison of methods. Tree Physiology, 20(16), 1113–1120.

Otukei, J.R. and Blaschke, T. 2010. Land cover change assessment using decision trees, support vector machines and maximum likelihood classification algorithms. International Journal of Applied Earth Observation and Geoinformation, 12, S27-S31.

Petropoulos, G. P., Kalaitzidis, C. and Vadrevu, K. P. 2012. Support vector machines and object-based classification for obtaining land-use/cover cartography from Hyperion hyperspectral imagery. Computers & Geosciences, 41, 99-107.

Pimentel, D., Lach, L., Zuniga, R. and Morrison, D. 2000. Environmental and economic costs of nonindigenous species in the United States. BioScience, 50, 53–65.

Porcar-Castell, A., Juurola, E., Ensminger, I., Berninger, F., Hari, P. and Nikinmaa, E. 2008. Seasonal acclimation of photosystem II in *Pinus sylvestris*. II. Using the rate constants of sustained thermal energy dissipation and photochemistry to study the effect of the light environment. Tree Physiology, 28(10), 1483–1491.

Rouse, J.W., Haas, R.H., Schell, J.A. and Deering, D.W. 1974. Monitoring vegetation systems in the Great Plains with ERTS. NASA Special Publication, 351, 309.

Saikia, P., Deka, J., Bharali, S., Kumar, A., Tripathi, O.P., Singha, L.B., Khan, M.L. and Dayanandan, S. 2017. Plant Diversity Patterns and Conservation Status of Eastern Himalayan Forests in Arunachal Pradesh, Northeast India. Forest Ecosystem, 4(1), 1-12,

Steyn, W.J., Wand, S.J.E., Holcroft, D.M. and Jacobs, G. 2002. Anthocyanins in vegetative tissues: a proposed unified function in photoprotection. New Phytologist, 155(3), 349–361.

Treitz, P.M. and Howarth, P.J. 1999. Hyperspectral remote sensing for estimating biophysical parameters of forest ecosystems. Progress in Physical Geography, 23(3), 359-390.

Ustin, S.L., Roberts, D.A., Gamon, J.A., Asner, G.P. and Green, R.O. 2004. Using imaging spectroscopy to study ecosystem processes and properties. BioScience, 54(6), 523–534.

Vogelmann, J.E., Rock, B.N. and Moss, D.M. 1993. Red edge spectral measurements from sugar maple leaves. International Journal of Remote Sensing, 14(8), 1563-1575.

Vyas, D., Krishnayya, N.S.R., Manjunath, K.R., Ray, S.S. and Panigrahy, S. 2011. Evaluation of classifiers for processing Hyperion (EO-1) data of tropical vegetation. International Journal of Applied Earth Observation and Geoinformation, 13(2), 228-235.

Whitmore, T.C. and Burslem, D. 1998. Major disturbances in tropical rainforests. pp. 549–565. In: Newbery, D.M., Prins, H.H.T. and Brown, N.D. (Eds.), Dynamics of Tropical Communities, Blackwell Science, Oxford,

Wilcove, D.S. and Chen, L. 1998. Management costs for endangered species. Conservation Biology, 12(6), 1405–1407.

Woolley, J. T. 1971. Reflectance and transmittance of light by leaves. Plant physiology, 47(5), 656–662.

Zarco-Tejada, P.J., Hornero, A., Beck, P.S.A., Kattenborn, T., Kempeneers, P. and Hernández-Clemente, R. 2019. Chlorophyll content estimation in an open-canopy conifer forest with Sentinel-2A and hyperspectral imagery in the context of forest decline. Remote Sensing of Environment, 223, 320-335.

Zarco-Tejada, P.J., Hornero, A., Hernández-Clemente, R. and Beck, P.S.A. 2018. Understanding the temporal dimension of the red-edge spectral region for forest decline detection using high-resolution hyperspectral and Sentinel-2a imagery. ISPRS Journal of Photogrammetry and Remote Sensing, 137, 134–14.

Received:4th August 2021
Accepted:19th February 2022